Seasonality in governing upper-ocean dynamics at submesoscales

Cesar, Sarah, Teri, & Bill[1]

Key Points.

- Submesoscale (10-100 km) vertical vorticity and horizontal divergence divergence undergo a strong seasonal cycle that are out-of-phase.
- Quasi-balanced turbulence dominates the variability in late Winter/early Spring; inertia-gravity waves dominate in late Summer/early Fall.
- These results have implications for the diagnosis of surface velocity from high-resolution altimeters.

(Type abstract here)

1. Introduction

Recent interest in upper-ocean dynamics has focused on the strong seasonal cycle of shallow baroclinic instabilities and their role in submesoscale (1-100 km) turbulence and mesoscale modulation [*Sasaki et al.*, 2014; *Qiu et al.*, 2014; *Callies et al.*, 2015; *Thompson et al.*, 2016; *Buckingham et al.*, 2016]. Contemporary studies have also suggested that inertia-gravity waves contribute significantly to the near-surface variability at scale submesoscales [*Richman et al.*, 2012; *Bühler et al.*, 2014; *Rocha et al.*, 2016].

Using the output of a 1/24° global simulation, we show that the near-surface expression of inertia-gravity waves undergo strong seasonal cycle that is out-of-phase with the seasonal cycle of the balanced variability. This seasonal cycle is associated with changes in the upper-ocean stratification. Consistent with previous studies, deep late Winter mixed-layers are prone to shallow baroclinic instabilities that are roughly in geostrophic balance and flux energy upscale [*Sasaki et al.*, 2014; *Callies et al.*, 2016], driving a mild seasonal modulation of the mesoscales [*Sasaki et al.*, 2014; *Qiu et al.*, 2014]. The horizontally divergent part of the flow, however, peaks in late Summer/early Fall, when the upper-ocean is strongly stratified. Hence these results suggest a strong seasonal modulation of the dominant upper-ocean submesoscale dynamics: quasi-balanced turbulence in late Winter/early Spring and quasi-linear inertia-gravity waves in late Summer/early Fall.

2. The LLC2160 model output

We use the output of a latitude-longitude polar cap (LLC) MITgcm numerical simulation [*Forget et al.*, 2015]. The output analyzed here, the LLC2160, is the 1/24° — 90-vertical-levels simulation from a hierarchy of global forward numerical solutions on a LLC grid that were spun up from a ECCO2 adjoint-method state estimate. The LLC2160 was forced by tides and 6-hourly surface fluxes similarly to the LLC4320 simulation used by *Rocha et al.* [2016] — see their appendix D. We chose the second-higher resolution simulation (LLC2160) of the LLC hierarchy because it was run for longer: the LLC2160 output spans two years form March 2011 to April 2013. The model timestep was 45s and the model variables were saved hourly. LLC hierarchy setup and control files are available online (at `http://mitgcm.org/viewvc/MITgcm/MITgcm_contrib/llc_hires`). For the LLC hierarchy, the sea-surface height is calculated using a linearized equation. While the nominal horizontal resolution of the LLC2160 simulation is 1/24°, horizontal wavenumber spectra suggests an effective resolution of about 20 km. (see figure 3).

A key aspect of the simulation analyzed here is that it is forced by the 16 most significant tidal components. Barotropic tides interact with topography and generate internal tides that project on mesoscales to submesoscales [*Rocha et al.*, 2016]. Hence, tidal forcing fundamentally distinguishes our analysis from recent modeling studies that investigated upper dynamics and its seasonality [*Sasaki et al.*, 2014; *Qiu et al.*, 2014].

The region of focus is the northwest Pacific, in the vicinities of the Kuroshio Extension, where previous studies have shown strong seasonality in the quasi-gesotrophic surface velocity field. We analyze a sub-domain of the LLC2160 simulation of about 2000 km^2 spanning 155-175°E; 25-40°N (figure 1a-b).

3. Seasonality in surface velocity and near-surface stratification

Focusing on the submesoscale variability, we present estimates of bulk quantities associated with the the horizontal velocity lateral gradient. The lateral gradients are calculated using a centered second-order finite differences scheme. We then calculate the vertical vorticity $\zeta \equiv v_x - u_y$ and horizontal divergence $\delta \equiv u_x + v_y$. These quantities highlight the submesoscale structures in the flow and hint on their dynamics.

Figures 1a-b show snapshots of vertical vorticity ζ in early Spring (April 15) and Fall (October 15). Clearly, a strong seasonality in vorticity exists: large values of fine-grained vertical vorticity are observed in early Spring with maximum values as high as $0.9f$, where f is the local planetary vorticity, and root-mean-square (RMS) of about 0.25. In early Fall, the situation is the opposite: the vertical vorticity is coarse-grained, and its local maximum and RMS is no larger than $0.3f$ and $0.1f$, respectively. Indeed, the seasonal cycle in vorticity/strain is very strong (Figure 2): the RMS vertical vorticity is about twice as large in late Winter/early Spring than it is in late Summer/early Fall. This picture is consistent with recent studies: shallow baroclinic instabilities energize the submesoscales in late Winter, drawing from the available potential energy stored in deep mixed layers [*Sasaki et al.*, 2014; *Callies et al.*, 2015, 2016].

The bulk of the vertical vorticity is associated with subinertial flows ($T_f = 2\pi/f_0 \approx 23.5$h, where f_0 is the inertial frequency at the mean latitude): daily-averaging the velocity fields reduces the vertical vorticity by less than 20% and the seasonal cycle remains strong (see green lines in figure 2). Most of this seasonal cycle is associated with submesoscale flows: smoothing the velocity field with a cut-off scale of 100 km reduces the RMS vorticity by at least 40%, yielding bulk statistics of velocity gradient roughly consistent with AVISO geostrophic velocities (see lines blue and black in figure 2).

The horizontal divergent part of the flow is significant: the RMS is $\delta/f > 0.1$). Most of these horizontal divergent flows are supra-inertial and project on scales smaller than

100 km: daily-averaging or smoothing the velocity fields (100 km cutoff) reduces the horizontal divergence by about 70%. Furthermore, the seasonal cycle in horizontal divergence is out-of-phase with the seasonal cycle of vertical vorticity: the horizontal divergence is about 30% larger in late Summer/early Fall than it is in late Winter/early Spring. The divergence associated with submesoscale subinertial eddies is small and its seasonal cycle is in phase with that of vorticity (see green lines). The seasonal cycle of the horizontal divergence is roughly in phase with the seasonal cycle of the near-surface (0-50m) stratification.

[1]Scripps Institution of Oceanography, University of California San Diego, La Jolla, CA, USA

0094-8276/16/$5.00

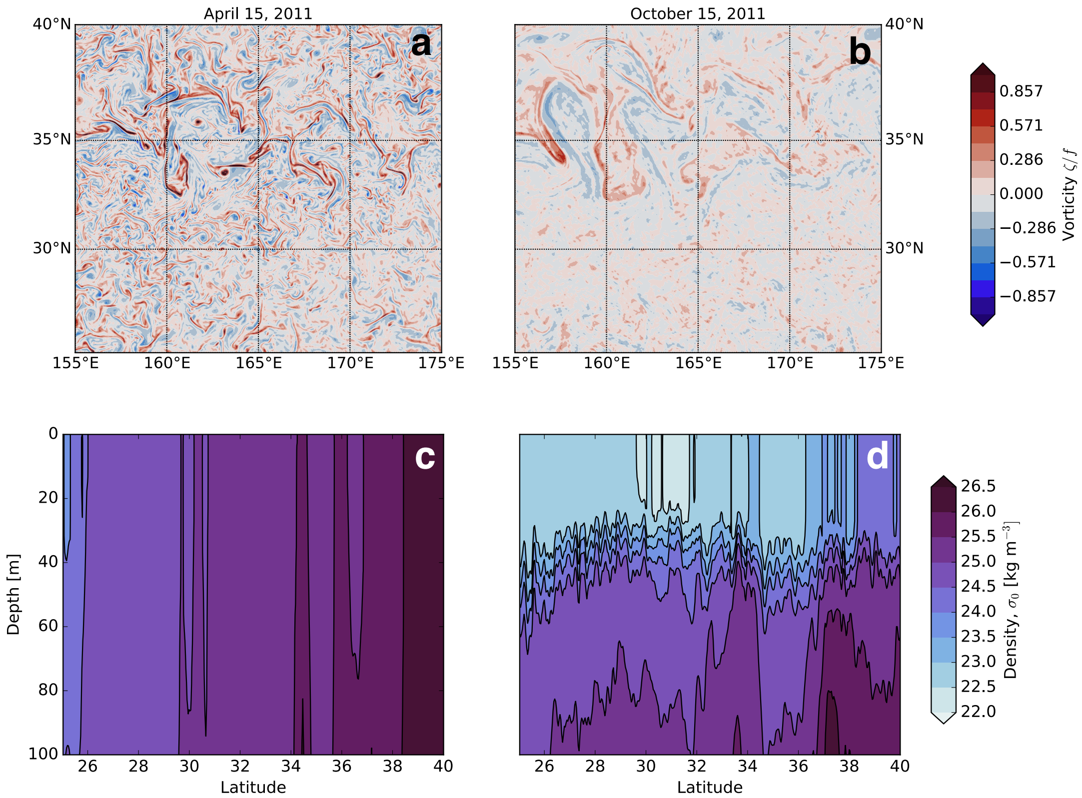

Figure 1. Snapshots of surface vorticity (a and b) and a transect of potential density at 165°E (c and d). The snapshots were taken at 00:00 UTC.

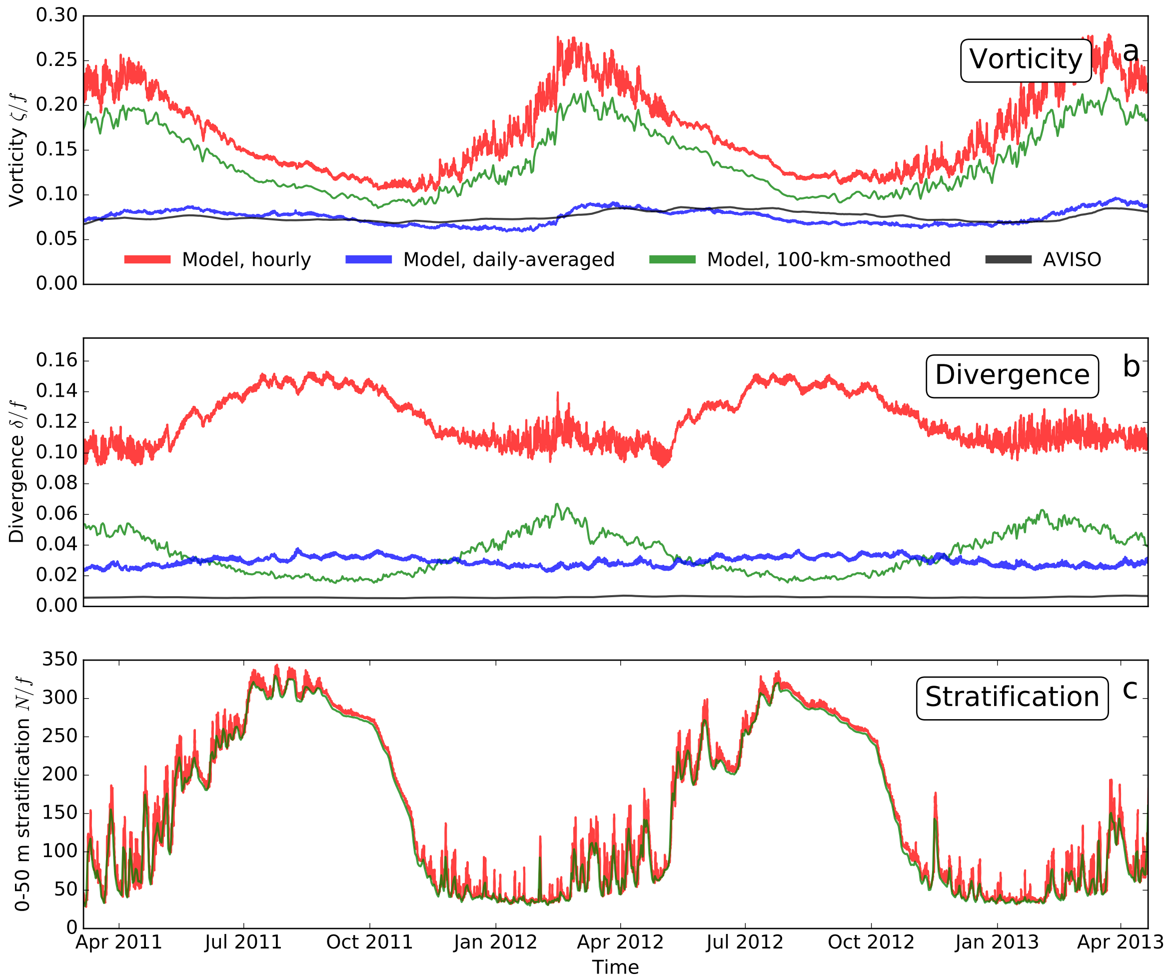

Figure 2. Time series of the root-mean-square of vorticity (a), horizontal divergence (b), and stratification in the upper 50 m (c). May add a time series of baroclinic production $\overline{w'b'}$ in the mixed layer. .

4. Projection on horizontal scales

To better understand the projection of these flows onto different horizontal scales, we calculate wavenumber spectra of kinetic energy and sea-surface height (SSH) variance. For simplicity we calculate zonal wavenumber spectra at various latitudes. The two-year time averaged and spatial linear trend were removed before calculating discrete Fourier transforms.Statistical significance is obtained by averaging over latitude and time. Using conservative temporal and spatial decorrelation estimate of 10 days and 250 km, we obtain roughly 50 independent realizations of the spectra.

Figure 3a depicts the horizontal wavenumber spectra of surface KE in April and October. At scales larger than 20km, the spectra based on hourly velocity snapshots are nearly indistinguishable within 95% confidence level (compare solid lines in figure 3a). Consistent with the results of *Rocha et al.* [2016] who analyzed the LLC4320 output in Drake Passage, there is significant high-frequency variabilty at submesoscales. Daily-averaging the velocity field suppresses spatial variability at scales small than about 250 km both in April and October (compare solid lines against dashed lines in figure 3a). But this suppression is more dramatic in October, when the horizontally divergent flows peak. At scales smaller than 100 km, 40% of the surface KE in April a is accounted for by suprainertial flows as opposed to 77% in October. The seasonality of subinertial submesoscale flows is significant, consistent with the results of *Sasaki et al.* [2014], which are based on snapshots of a model without tidal forcing.

These high-frequency submesoscale flows significantly project on the sea-surface. In October, when the horizontally divergent flows peak and the submesoscale balanced flows are minimum, there is a dramatic difference between the spectra based on hourly and daily-averaged SSH: at scales smaller than 100 km, the spectra of hourly SSH roughly follows a -2 power-law, whereas the spectra of daily-averaged SSH roughly follows a -5 power-law. At scales smaller than 100 km, 44% of the surface KE in April is accounted for by suprainertial flows as opposed to 86% in October! The out-of-phase seasonal cycle of subinertial and suprainertial flows conspire to yield no significant seasonality in the spectra of hourly SSH.

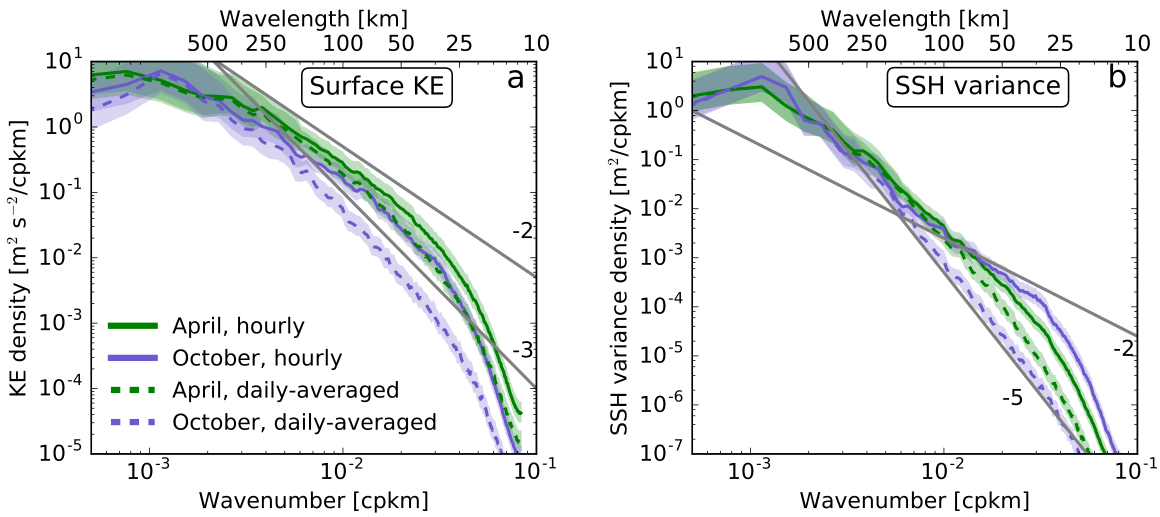

Figure 3. Surface (horizontal) KE and SSH variance wavenumber spectra. Solid lines are spectra based on hourly snapshots, dashed lines are spectra based on daily-averaged fields.

5. Projection on time scales

To better understand the high-frequency/high-wavenumber flows we calculate frequency spectra of surface KE (figure 4). To obtain statistically meaningful results, we average spectral estimates along a section at 165°E. There is about 50 independent spectral realizations.

The surface KE spectra of subinertial flows very roughly follow a -2 power-law. The high-frequency flows are split near-inertial flows, tidal signals and their higher harmonics. Hence these high-frequency flows are dominated by inertia-gravity waves. (Note that the inertial peak nearly merges with the diurnal tide peak.) There is statistically significant seasonality. The seasonal cycle of the sub-inertial motions (at least for periods between 5-20 days) is out-of-phase with the seasonal cycle of supra-inertial flows: the former are more energetic in April and the latter in October.

Most of these high-frequency inertia-gravity waves project onto scales smaller than 100 km. The surface KE spectra of 100-km-smoothed velocity field is significantly suppressed in supra-inertial frequencies — there are no statistically significant changes at sub-inertial frequencies (see dashed lines in figure 4).

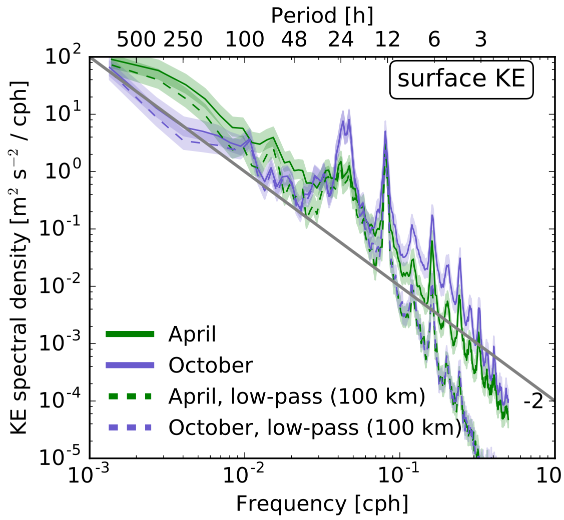

Figure 4. Surface (horizontal) KE frequency spectra. Solid lines are spectra based on the 1/24° fields, dashed line are spectra based on 100-km-smoothed fields.

6. Summary and Discussion

Our main finding is that upper-ocean divergent flows, dominated by inertia-gravity waves, undergo a strong seasonal cycle that is out-of-phase with the seasonal cycle of the quasi-balanced flows. Therefore, the present results suggest significant seasonal modulation of the dominant upper-ocean dynamics at submesoscales (10-100 km): quasi-balanced turbulence driven by shallow baroclinic instabilities in late Winter/early Spring and inertia-gravity waves dominate in late Summer/early Fall.

That the surface velocity and SSH submesoscale (10-100 km) variability may be dominated by ageostrophic flows in Summer/Fall has consequences for the interpretation of data from the future SWOT and COMPIRA altimeter missions, which will deliver SSH measurements at submesoscales. To the extent that high-frequency flows are dominated by spatially incoherent internal tides and other internal waves, it may be very difficult (if not impossible) to separate submesoscale SSH variability associated with geostrophic motions from high-frequency, ageostrophic flows. Thus, previous claims that one will be able to easily obtain submesoscale surface geostrophic velocities and monitor such seasonal cycle on global scales [*Sasaki et al.*, 2014; *Qiu et al.*, 2014] are overstated.

The present analysis focuses on a single patch of ocean in the vicinities of the Kuroshio Extension, not representative of other regions such as eastern boundary currents and the middle of the subtropical gyre: care must be taken in overgeneralizing these results. The effects of smaller-scale/higher-frequency "sub-submesoscale" flows on the submesoscale surface velocity and SSH variability are presently unknown.

Appendix A: How well does the model captures high-frequency modes?

To assess how well the LLC2160 represents the high-frequency variability, we compare the model near-surface velocity field against two available mooring data: KEO (the data is available online at `http://www.pmel.noaa.gov/ocs/KEO`) and KESS mooring #7 (the data is available online at `http://uskess.whoi.edu`). For proper comparison, we use model data closest to these two moorings (west of the region considered in the present study). Focusing on high-frequencies, we calculate frequency spectral estimates every month. There are about 48 independent spectral realizations.

Figure 5 shows KE frequency spectra for the model and mooring data. At the uppermost common depth (20 m), very low frequencies (periods ¿ 10 days) and the inertial, diurnal, and semi-diurnal frequencies agree well — the KESS data are more energetic at intermedia frequencies. At 40 m, the model and observations have consistent spectra at periods larger than about 6 h. The data from moorings are more energetic at higher frequencies and tidal harmonics are not observed, except for the first two harmonics that are apparent in the KESS data at 40 m. Three reasons for the lack of tidal harmonics in the mooring data are: 1) The high- frequency variability is dominated by high-frequency noise due to mooring vertical excursions; 2) The model does not have enough resolution to resolve the full spectrum of ultraviolet catastrophic wave-wave interactions; 3) The model is not forced at frequencies higher that 6h.

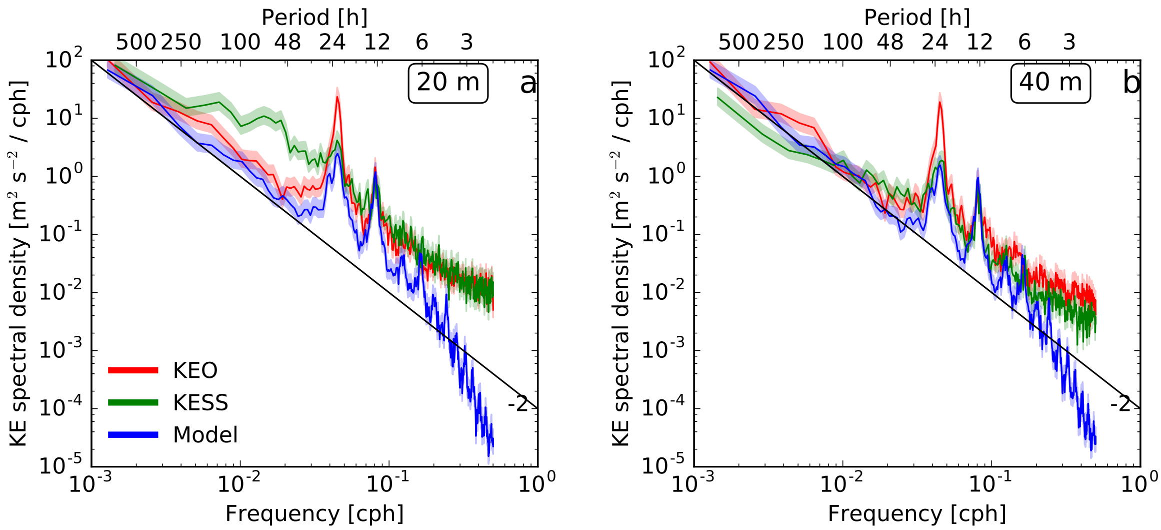

Figure 5. A near-surface KE spectra comparison between model and two available mooring observations.

Acknowledgments. Thanks to D. Menemenlis (JPL/NASA) and the other MITgcm usual suspects. This research was funded by NSF and NASA.

References

Buckingham, C. E., A. C. Naveira Garabato, A. F. Thompson, L. Brannigan, A. Lazar, D. P. Marshall, A. George Nurser, G. Damerell, K. J. Heywood, and S. E. Belcher (2016), Seasonality of submesoscale flows in the ocean surface boundary layer, *Geophysical Research Letters*, *43*(5), 2118–2126.

Bühler, O., J. Callies, and R. Ferrari (2014), Wave–vortex decomposition of one-dimensional ship-track data, *Journal of Fluid Mechanics*, *756*, 1007–1026.

Callies, J., R. Ferrari, J. M. Klymak, and J. Gula (2015), Seasonality in submesoscale turbulence, *Nature communications*, *6*.

Callies, J., G. Flierl, R. Ferrari, and B. Fox-Kemper (2016), The role of mixed-layer instabilities in submesoscale turbulence, *Journal of Fluid Mechanics*, *788*, 5–41.

Forget, G., J.-M. Campin, P. Heimbach, C. Hill, R. Ponte, and C. Wunsch (2015), Ecco version 4: an integrated framework for non-linear inverse modeling and global ocean state estimation, *Geosci. Model Dev.*, *8*, 3071–3104.

Qiu, B., S. Chen, P. Klein, H. Sasaki, and Y. Sasai (2014), Seasonal mesoscale and submesoscale eddy variability along the north pacific subtropical countercurrent, *Journal of Physical Oceanography*, *44*(12), 3079–3098.

Richman, J. G., B. K. Arbic, J. F. Shriver, E. J. Metzger, and A. J. Wallcraft (2012), Inferring dynamics from the wavenumber spectra of an eddying global ocean model with embedded tides, *Journal of Geophysical Research: Oceans*, *117*(C12).

Rocha, C. B., T. K. Chereskin, S. T. Gille, and D. Menemenlis (2016), Mesoscale to submesoscale wavenumber spectra in drake passage, *Journal of Physical Oceanography*, *46*, 601–620.

Sasaki, H., P. Klein, B. Qiu, and Y. Sasai (2014), Impact of oceanic-scale interactions on the seasonal modulation of ocean dynamics by the atmosphere, *Nature communications*, *5*.

Thompson, A. F., A. Lazar, C. Buckingham, A. C. Naveira Garabato, G. M. Damerell, and K. J. Heywood (2016), Open-ocean submesoscale motions: A full seasonal cycle of mixed layer instabilities from gliders, *Journal of Physical Oceanography*, *46*(4), 1285–1307.